X-ray Spectroscopy of QSOs with Broad Ultraviolet Absorption Lines

S. C. Gallagher, W. N. Brandt, G. Chartas, and G. P. Garmire
Department of Astronomy and Astrophysics
The Pennsylvania State University
University Park, PA 16802
USA
gallsc, niel, chartas, garmire@astro.psu.edu

ABSTRACT

For the population of QSOs with broad ultraviolet absorption lines, we are just beginning to accumulate X-ray observations with enough counts for spectral analysis at CCD resolution. From a sample of eight QSOs [including four Broad Absorption Line (BAL) QSOs and three mini-BAL QSOs] with *ASCA* or *Chandra* spectra with more than 200 counts, general patterns are emerging. Their power-law X-ray continua are typical of normal QSOs with $\Gamma \approx 2.0$, and the signatures of a significant column density [$N_{\rm H} \approx (0.1\text{–}4)\times10^{23}\,{\rm cm}^{-2}$] of intrinsic, absorbing gas are clear. Correcting the X-ray spectra for intrinsic absorption recovers a normal ultraviolet-to-X-ray flux ratio, indicating that the spectral energy distributions of this population are not inherently anomalous. In addition, a large fraction of our sample shows significant evidence for complexity in the absorption. The subset of BAL QSOs with broad Mg II absorption apparently suffers from Compton-thick absorption completely obscuring the direct continuum in the 2–10 keV X-ray band, complicating any measurement of their intrinsic X-ray spectral shapes.

Subject headings: galaxies: active — quasars: absorption lines — X-rays: galaxies

1. Introduction

Since the first surveys with *ROSAT*, Broad Absorption Line (BAL) QSOs have been known to have faint soft X-ray fluxes compared to their optical fluxes (Kopko, Turnshek, & Espey 1994; Green & Mathur 1996). Given the extreme absorption evident in the ultraviolet (UV), this soft X-ray faintness was assumed to result from intrinsic absorption. Based on this model, the intrinsic column densities required to suppress the X-ray flux, assuming a normal QSO spectral energy distribution, were found to be $\gtrsim 5\times10^{22}\,{\rm cm}^{-2}$ (Green & Mathur 1996). Due to the 2–10 keV response of its detectors, a subsequent *ASCA* survey was able to raise this lower limit for some objects by an order of magnitude, to $\gtrsim 5\times10^{23}\,{\rm cm}^{-2}$ (Gallagher et al. 1999). In all of these studies, the premise of a typical underlying QSO spectral energy distribution and X-ray continuum was maintained. The strong correlation found by Brandt, Laor, & Wills (2000; hereafter BLW) between C IV absorption equivalent width (EW) and faintness in soft X-rays further supported this assumption.

ASCA observations of two BAL QSOs, PHL 5200 (Mathur et al. 1995) and Mrk 231 (Iwasawa 1999; Turner 1999), provided suggestive evidence that intrisic absorption was in fact to blame for X-ray faintness. However, the limited photon statistics and bandpass precluded a definitive diagnosis. The observation of PG 2112+059 with *ASCA* provided the first solid evidence for intrinsic X-ray absorption and a normal underlying X-ray continuum in a BAL QSO (Gallagher et al. 2001c). Subsequently, a few more observations of BAL QSOs with *ASCA* and *Chandra* have upheld this result (Green et al. 2001; Mathur et al. 2001; Gallagher et al. 2001b). Observations of three mini-

BAL QSOs,[1] PG 1411+442 (Brinkmann et al. 1999), RX J0911.4+0551 (Chartas et al. 2001), and PG 1115+080 (Gallagher et al. 2001a), were also consistent with the absorption scenario.

In this paper, we have gathered the results from the 0.5–10 keV spectral analyses of all the available QSOs with broad UV absorption lines, including BAL QSOs, mini-BAL QSOs, and one Narrow-Line Seyfert 1 galaxy, with more than 200 counts. Though additional data exist in the literature, these are the only sources with enough counts for spectral analysis on an individual basis. From our experience, drawing strong conclusions about the nature of an X-ray spectrum based on fewer counts can lead to interpretations that are not upheld by higher quality data.

2. Sample Data

Our sample is listed in Table 1, along with some relevant observational parameters. The X-ray data were taken by the *ASCA* and *Chandra* observatories, as indicated in the "Notes" column to Table 1, and Figure 1 shows those spectra not previously published. The analyses for the sample objects are described in the references listed in Table 1, with the exceptions of PG 1411+442 (Brinkmann et al. 1999) and PHL 5200 (Mathur et al. 2001). The spectral analyses for these two objects have been redone according to the method detailed in Gallagher et al. (2001c) to ensure consistency with the other results. For PHL 5200, corrective measures for dealing with the degradation of the *ASCA* CCD detectors, as outlined in Weaver, Gelbord, & Yaqoob (2000; Appendix A), were followed. Our derived photon index for the underlying X-ray power-law continuum pf PHL 5200, $\Gamma = 2.17^{+0.60}_{-0.47}$, was significantly flatter than that of the preferred model of Mathur et al. (2001).

The general strategy for all of the X-ray analysis was to first try to fit the data with a simple power-law model (including Galactic absorption) and subsequently add intrinsic absorption of three sorts: neutral, partially covering neutral, and ionized. In all cases, including intrinsic absorption provided statistically acceptable models and improved the χ^2 of the fits significantly. For the gravitational lenses, APM 08279+5255, RX J0911.4+0551, PG 1115+080, and H 1413+117, the lensing galaxies could provide some of the observed absorption. However, this contribution is unlikely to be significant. At the redshifts of the known lenses, the column density would have to be $\gtrsim 10^{22}$ cm^{-2}, much larger than the typical $N_{\rm H}$ through the outer regions of a galaxy, to affect strongly the best-fitting column density. In general, distinguishing between a partially covering and ionized absorber is not possible statistically; with CCD resolution and the current statistics, the two models can fit the data equally well. Typically, the ionized-absorber models produce column densities within a factor of 0.5–2.0 of the partial-covering models. However, though an ionized absorber was included for completeness in fitting each of the spectra, the ionized-absorber models, such as absori in the spectral fitting package XSPEC (Arnaud 1996), assume a single-zone, optically thin plasma. Such assumptions are not in general appropriate for the large X-ray column densitities, $N_{\rm H}\gtrsim 10^{22}\,{\rm cm}^{-2}$, exhibited by QSOs with broad UV absorption (H. Netzer, 2001, priv. comm.). Therefore, when a complex absorber model provided a statistically significant improvement over a simple neutral absorber, the partial-covering model was chosen.

The column densities and covering fractions for the best-fitting absorption models, as well as the best-fitting photon indices, are listed in Table 1.

3. Results

As obtaining even moderate-quality spectra of these faint X-ray sources requires a significant amount of observing time with the current generation of X-ray observatories, a comprehensive and intricate X-ray picture of the population of QSOs with broad UV absorption lines awaits the accumulation of a significantly larger body of data. However, as the number of these QSOs observed in X-rays grows, a consistent basic picture is beginning to emerge.

3.1. Normal Underlying QSO Continua

Most fundamentally, the days of assuming, without evidence, that QSOs with broad UV absorption lines have the underlying X-ray continua

[1] Mini-BAL QSOs contain UV absorption lines with velocity widths of $\sim 10^3$ km s^{-1}, but they do not formally meet the BAL QSO criteria established by Weymann et al. (1991).

of normal QSOs are over. The spectroscopic measurement of the photon index, Γ, of the power-law continuum for each of these objects versus redshift is shown in Figure 2a. Excluding the apparent outlier H 1413+117, the mean photon index for our sample is $\Gamma = 2.01 \pm 0.13$, entirely consistent with the range of Γ measured for large samples of low and high luminosity radio-quiet QSOs (**?**, e.g.,)]GeEtal2000,ReTu2000. Furthermore, there is no evidence for strong systematic changes in spectral slope as a function of redshift. In fact, the well-measured continuum slope of APM 08279+5255 ($\Gamma = 1.86^{+0.26}_{-0.23}$) extends constraints on radio-quiet QSO X-ray continuum shape evolution to significantly higher redshift, $z = 3.87$, than previously possible.

For evaluating the spectral energy distribution of a QSO, the quantity $\alpha_{\rm ox}$ measures the relative flux densities at 2 keV and 3000 Å. Radio-quiet QSOs without intrinsic absorption have $\alpha_{\rm ox} = -1.51 \pm 0.14$ (BLW), while absorbed QSOs tend to have $\alpha_{\rm ox} \lesssim -1.7$. The $\alpha_{\rm ox}$ values for this sample are found to be generally indicative of absorption (see Table 1 and Figure 2b), though the measured X-ray column-density is not obviously correlated with $\alpha_{\rm ox}$. Though our values for the 3000 Å flux density were not corrected for possible intrinsic reddening, this is not expected to be a significant problem for these blue QSOs. Furthermore, though variability between the optical and X-ray observations could result in an inaccurate $\alpha_{\rm ox}$, this quantity is only sensitive to large changes in flux density; e.g., a factor of two increase in the 3000 Å flux density only corresponds to $\Delta\alpha_{\rm ox} = 0.1$. Correcting the X-ray spectra for the fitted intrinsic absorption brings these objects within the range of typical $\alpha_{\rm ox}$, indicating that the underlying spectral energy distributions are not anomalous (see Figure 2b). Both of the assumptions of the early BAL QSO X-ray work, normal X-ray continuum and typical $\alpha_{\rm ox}$, are thus supported.

3.2. Complex Absorption

A simple neutral absorber blocks almost all X-ray flux up to an energy set by the column density; for $N_{\rm H} = 10^{23}\,{\rm cm}^{-2}$, X-rays up to ~ 3 keV in the rest frame are absorbed. A signature of more complex absorption, for example partial covering and/or ionized gas along the line of sight, is a much less abrupt decline of the flux at the lowest energies (see Figure 1b for an example). For five of the eight sources, a partial-covering absorber provided a statistically significant improvement over a neutral absorber, and the column densities listed are for that model.

For the remaining three QSOs, APM 08279+5255, H 1413+117, and PG 2112+059, the current data do not permit the nature of the absorber to be examined in detail. For H 1413+117 and PG 2112+059, the signal-to-noise ratio of the X-ray data below 1 keV is insufficient for studying the structure of the absorption, and for APM 08279+5255, the large redshift ($z = 3.87$) pushes the signatures of a complex absorber below the *Chandra* ACIS bandpass (0.5–8.0 keV).

3.2.1. H 1413+117

The famous gravitationally lensed "Cloverleaf" QSO, H 1413+117, does not fit within the basic picture outlined above for the other absorbed QSOs in this sample. Though significant intrinsic absorption is measured, the best-fitting photon index is unusually flat for a radio-quiet QSO, $\Gamma \approx 1.4$. Furthermore, even after correcting for intrinsic absorption, $\alpha_{\rm ox}$ remains low at -1.74. Finally, including a narrow, 6.4 keV Fe Kα emission line in the model improves the fit at the $> 99\%$ confidence level according to the F-test ($\Delta\chi^2 = 9.1$ for one additional fitting parameter; Figure 1c). In the rest frame, this strong line has an equivalent width of EW $= 650^{+354}_{-517}$ eV. The flat rest-frame 1.8–18 keV slope and strong Fe Kα emission line together suggest that the spectrum is reflection-dominated, and thus the direct X-rays are completely obscured. In terms of absorption-line profiles, H 1413+117 is similar to PHL 5200, with smooth profiles starting at near-zero velocities (Turnshek et al. 1988), and both QSOs also exhibit high continuum polarization (Goodrich & Miller 1995). However, the X-ray properties of these two QSOs are quite different as PHL 5200 shows no evidence for reflection. The difference between H 1413+117 and the other BAL QSOs may lie in its UV spectrum; Hazard et al. (1984) found broad Al III absorption, which has never been found without Mg II absorption, the signature of a low-ionization BAL QSO (LoBAL QSO; N. Arav and M. Brotherton 2001, priv. comm.).

Those BAL QSOs with broad absorption

in Mg II have notably lower α_{ox} values than BAL QSOs with only high-ionization absorption lines (Gallagher et al. 1999; Green et al. 2001). This could plausibly result from either an intrinsically X-ray weak continuum, or from heavy, perhaps Compton-thick, obscuration (**?**, e.g.,)]GrEtal2001. In the latter case, only indirect X-rays from the active nucleus, either scattered around the obscuration by a small-scale electron mirror or reflected off of more distant, neutral material, can reach the observer, and the intrinsic X-ray power of the nucleus cannot be directly measured. Given the extreme X-ray faintness of this class of objects, very few spectra are likely to be obtained. The two examples available at present are Mrk 231 (Maloney & Reynolds 2000; Gallagher et al. 2001b) and H 1413+117. For these two objects, two pieces of evidence indicate that the direct X-ray continuum is not being observed: the spectral shape is unusually flat ($\Gamma \lesssim 1.5$), and the value of α_{ox} is still low after correcting for all the direct signs of absorption.

4. Discussion

In every case where the analysis is sensitive to structure in the X-ray absorption, we find evidence for complexity. While we model this complexity as intrinsic, neutral absorption partially covering the X-ray continuum source, the actual nature of this absorbing gas could be much more complicated. X-ray scattering in the nucleus effectively causes partial-covering absorption, and if the X-ray absorbing gas is physically related to that absorbing the UV continuum, then it should also be ionized. Determining the ionization state of the X-ray absorbing gas and the continuum scattering fraction is essential for accurately measuring the column density. Furthermore, the current modeling assumes no velocity dispersion in the absorbing gas. In such gas, the opacity in the soft X-rays arises primarily from bound-free metal edges, and these are used to determine the absorption column density. With a significant velocity dispersion, the opacity of bound-bound absorption lines can increase significantly. Therefore, the assumption of zero velocity dispersion, clearly naïve for BAL QSOs, may result in an overestimate of the amount of X-ray absorbing gas.

The significant correlation found by BLW of C IV absorption EW versus weakness in soft X-rays holds across several orders of magnitude of absorption EW. The inference that the weakness in soft X-rays is the result of intrinsic absorption has been substantiated spectroscopically for all but one of the objects in our sample (H 1413+117, see § 3.2.1). However, directly identifying the EW of the UV absorption with the column density of the X-ray absorbing gas is problematic (see Figure 2c). BLW speculated that at the absorbed end of their correlation, the EW of C IV is dominated primarily by velocity dispersion rather than column density. In this case, BAL QSOs, by definition (Weymann et al. 1991), would be expected to have the most extreme C IV EW properties, as they do. As seen in Figure 2c though, BAL QSOs may not necessarily always have the largest X-ray absorption column densities.

In terms of gross X-ray properties, it has become apparent that drawing a distinction between BAL QSOs and other QSOs with broad UV absorption lines is largely a matter of semantics. The photon indices and the column densities measured with the current X-ray observatories overlap. Future, higher spectral resolution X-ray observations may reveal features warranting separate classifications, but at present the differences do not justify treating the BAL and mini-BAL QSO populations, for example, as distinct.

5. Future Work

Though X-ray spectroscopy of QSOs with broad UV absorption lines is finally addressing some of the questions first raised by *ROSAT* observations, many issues remain unresolved. Primarily, the velocity structure and ionization state of the X-ray absorbing gas are unknown. Without this crucial information, the mass ejection rate of gas from the nuclei of these QSOs cannot be determined. This parameter is fundamental for understanding the balance of accretion and outflow in the central engine. To address these important questions, X-ray spectroscopy at gratings resolution of the X-ray brightest QSOs with broad UV absorption is the next step. Investigating the physical basis for the extreme X-ray faintness of LoBAL QSOs may need to await the next generation of X-ray observatories.

We thank F. Hamann for providing equivalent-width data, C. Vignali for helpful discussions, and M. Brotherton for constructive comments that improved this paper. NASA grant NAS 8-38252, P.I. GPG, supports the ACIS instrument team. SCG gratefully acknowledges support from NASA GSRP grant NGT5-50277 and from the Pennsylvania Space Grant Consortium. WNB thanks NASA LTSA grant NAG5-8107.

REFERENCES

Arnaud, K. A. 1996, in ASP Conf. Ser. 101, Astronomical Data Analysis Software and Systems V, ed. G. Jacoby & J. Barnes (San Francisco: ASP), 17

Bade, N., Siebert, J., Lopez, S., Voges, W., & Reimers, D. 1997, A&A, 317, L13

Brandt, W. N., Laor, A., & Wills, B. J. 2000, ApJ, 528, 637

Brinkmann, W., Wang, T., Matsuoka, M., & Yuan, W. 1999, A&A, 345, 43

Chartas, G., Dai, X., Gallagher, S. C., Garmire, G. P., Bautz, M. W., Schechter, P. L., & Morgan, N. D. 2001, ApJ, 558, 119

Ellison, S. L., Lewis, G. F., Pettini, M., Sargent, W. L. W., Chaffee, F. H., Foltz, C. B., Rauch, M., & Irwin, M. J. 1999, PASP, 111, 946

Gallagher, S. C., Brandt, W. N., Chartas, G., & Garmire, G. P. 2001a, in ASP Conf. Ser., Mass Outflow in Active Galactic Nuclei: New Perspectives, ed. D. M. Crenshaw, S. B. Kraemer, & I. M. George, Vol. in press (astro-ph/0105332) (San Francisco: ASP)

Gallagher, S. C., Brandt, W. N., Chartas, G., Garmire, G. P., & Sambruna, R. M. 2001b, ApJ, submitted

Gallagher, S. C., Brandt, W. N., Laor, A., Elvis, M., Mathur, S., Wills, B. J., & Iyomoto, N. 2001c, ApJ, 546, 795

Gallagher, S. C., Brandt, W. N., Sambruna, R. M., Mathur, S., & Yamasaki, N. 1999, ApJ, 519, 549

George, I. M., Turner, T. J., Yaqoob, T., Netzer, H., Laor, A., Mushotzky, R. F., Nandra, K., & Takahashi, T. 2000, ApJ, 531, 52

Goodrich, R. W., & Miller, J. S. 1995, ApJ, 448, L73

Green, P. J., Aldcroft, T. L., Mathur, S., Wilkes, B. J., & Elvis, M. 2001, ApJ, 558, 109

Green, P. J., & Mathur, S. 1996, ApJ, 462, 637

Hamann, F., Korista, K. T., & Morris, S. L. 1993, ApJ, 415, 541

Hazard, C., Morton, D. C., Terlevich, R., & McMahon, R. 1984, ApJ, 282, 33

Iwasawa, K. 1999, MNRAS, 302, 96

Kopko, M., Turnshek, D. A., & Espey, B. R. 1994, in IAU Symp. 159: Multi-Wavelength Continuum Emission of AGN, ed. T. Courvoisier & A. Blecha, Vol. 159 (Dordrecht: Kluwer), 450

Maloney, P. R., & Reynolds, C. S. 2000, ApJ, 545, L23

Mathur, S., Elvis, M., & Singh, K. P. 1995, ApJ, 455, L9

Mathur, S., Matt, G., Green, P. J., Elvis, M., & Singh, K. P. 2001, ApJ, 551, L13

Neugebauer, G., Green, R. F., Matthews, K., Schmidt, M., Soifer, B. T., & Bennett, J. 1987, ApJS, 63, 615

Reeves, J. N. & Turner, M. J. L. 2000, MNRAS, 316, 234

Turner, T. J. 1999, ApJ, 511, 142

Turnshek, D. A., Grillmair, C. J., Foltz, C. B., & Weymann, R. J. 1988, ApJ, 325, 651

Weaver, K. A., Gelbord, J., & Yaqoob, T. 2001, ApJ, 550, 261

Weymann, R. J., Morris, S. L., Foltz, C. B., & Hewett, P. C. 1991, ApJ, 373, 23

AAS LaTeX macros v5.0.

TABLE 1
BASIC PROPERTIES OF QSOS WITH BROAD ULTRAVIOLET ABSORPTION LINES

Name[a]	B	z	Intrinsic $N_{\rm H}$[b] ($10^{22}\,{\rm cm}^{-2}$)	Covering Fraction[b]	Γ[b]	$\alpha_{\rm ox}/\alpha_{\rm ox(corr)}$[c]	C IV EW[d] (Å)	Notes[e]
APM 08279+5255[1]	19.2	3.870	$6.0^{+3.5}_{-3.1}$	···	$1.86^{+0.26}_{-0.23}$	$-2.26/-1.70$[5]	21[5]	B, GL, C
RX J0911.4+0551[2]	18.0	2.800	19^{+28}_{-18}	$0.71^{+0.20}_{-0.39}$	$1.87^{+0.98}_{-0.66}$	$-1.72/-1.52$[6]	4.4[6]	mB, GL, C
PG 1115+080[1]	15.8	1.722	$3.8^{+2.5}_{-2.2}$	$0.64^{+0.12}_{-0.17}$	$1.99^{+0.26}_{-0.21}$	$-1.74/-1.60$[7]	···	mB, GL, C
H 1413+117[1]	17.0	2.548	20^{+18}_{-12}	···	$1.39^{+0.73}_{-0.61}$	$-2.17/-1.74$[8]	46[9]	B, GL, C
PG 1411+442[3]	15.0	0.090	$19^{+7.5}_{-6.6}$	$0.97^{+0.02}_{-0.12}$	$2.20^{+0.91}_{-0.90}$	$-2.01/-1.44$[7]	8.5[10]	mB, A
PG 1535+547[4]	15.3	0.038	12^{+8}_{-5}	$0.91^{+0.07}_{-0.26}$	$2.02^{+0.92}_{-0.95}$	$-2.03/-1.66$[7]	4.6[10]	NLS1, A
PG 2112+059[4]	15.5	0.457	$1.1^{+0.5}_{-0.4}$	···	$1.97^{+0.26}_{-0.23}$	$-1.62/-1.55$[7]	19[10]	B, A
PHL 5200[3]	18.0	1.981	40^{+26}_{-22}	$0.79^{+0.12}_{-0.23}$	$2.17^{+0.60}_{-0.47}$	$-1.66/-1.44$[8]	55[9]	B, A

[a]Numerical superscripts in this column indicate the reference for the detailed description of the X-ray analysis. [1]Chartas et al., in prep.; [2]Chartas et al. (2001); [3]see §2; [4]Gallagher et al. (2001a).

[b]Errors are given for 90% confidence taking all parameters except normalization to be of interest.

[c]The values for $\alpha_{\rm ox(corr)}$ were calculated from the X-ray spectrum corrected for intrinsic absorption. Numerical superscripts indicate the references for the 3000 Å flux densities used to calculate $\alpha_{\rm ox}$ and $\alpha_{\rm ox(corr)}$. [5]Ellison et al. (1999); [6]Bade et al. (1997); [7]Neugebauer et al. (1987); [8]Weymann et al. (1991).

[d]Sources of C IV absorption EW values are indicated with numerical superscripts. [9]Hamann et al. (1993); [10]Brandt et al. (2000).

[e]Key: B: BAL QSO; mB: mini-BAL QSO; NLS1: Narrow-Line Seyfert 1; GL: gravitational lens. The sources of the data are *ASCA* (A) and *Chandra* (C).

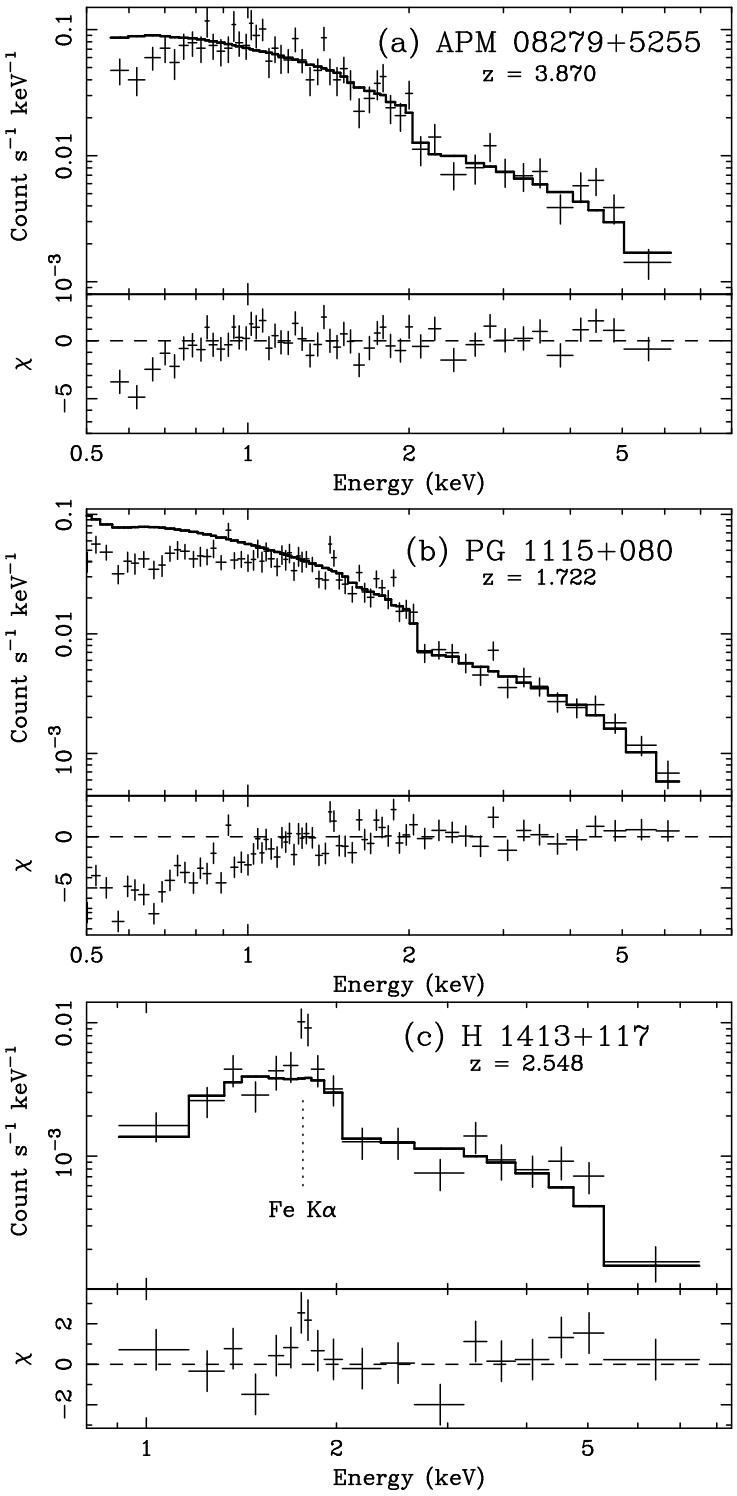

Fig. 1.— Observed-frame *Chandra* ACIS-S3 spectra. Both **(a)** APM 08279+5255 and **(b)** PG 1115+080 have been fit above rest-frame 5 keV with a power-law model that has then been extrapolated back to lower energies. The residuals at low energies are signatures of significant intrinsic absorption. **(c)** H 1413+117. The continuum has been fit with a power-law model with intrinsic absorption. Significant positive residuals near rest-frame 6.4 keV are indicative of a strong neutral Fe Kα emission line with rest-frame EW$\approx$ 650 eV.

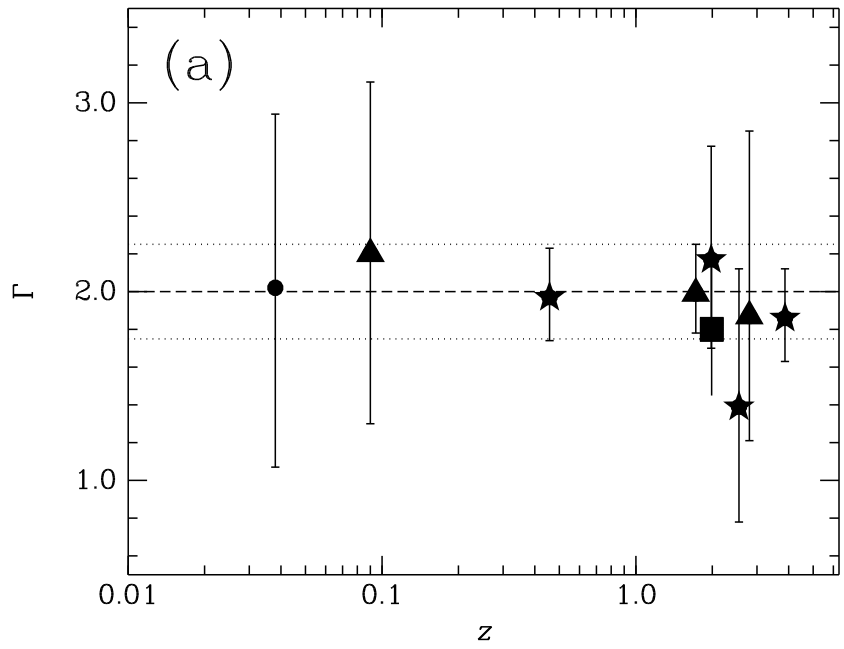

Fig. 2.— For all plots, data points are for the QSOs listed in Table 1 unless otherwise indicated. Filled stars mark BAL QSOs, filled triangles mark mini-BAL QSOs, and the filled circle marks the NLS1, PG 1535+547. **(a)** Photon index versus redshift for the QSOs listed in Table 1. The filled square is the result from Green et al. (2001) for a simultaneous fit to six BAL QSOs versus their median z. The dashed line represents the mean of the George et al. (2000) *ASCA* sample of radio-quiet QSOs, and the dotted lines indicate the dispersion. **(b)** Histograms of $\alpha_{\rm ox}$ values. The dotted histogram shows the distribution of the BLW sample of low-redshift Palomar-Green QSOs without known X-ray absorption. The shaded histogram shows the distribution of $\alpha_{\rm ox}$ for our sample as listed in Table 1. The filled symbols show $\alpha_{\rm ox(corr)}$, the $\alpha_{\rm ox}$ values for our sample corrected for intrinsic X-ray absorption. **(c)** Intrinsic X-ray column density versus rest-frame C IV absorption EW.

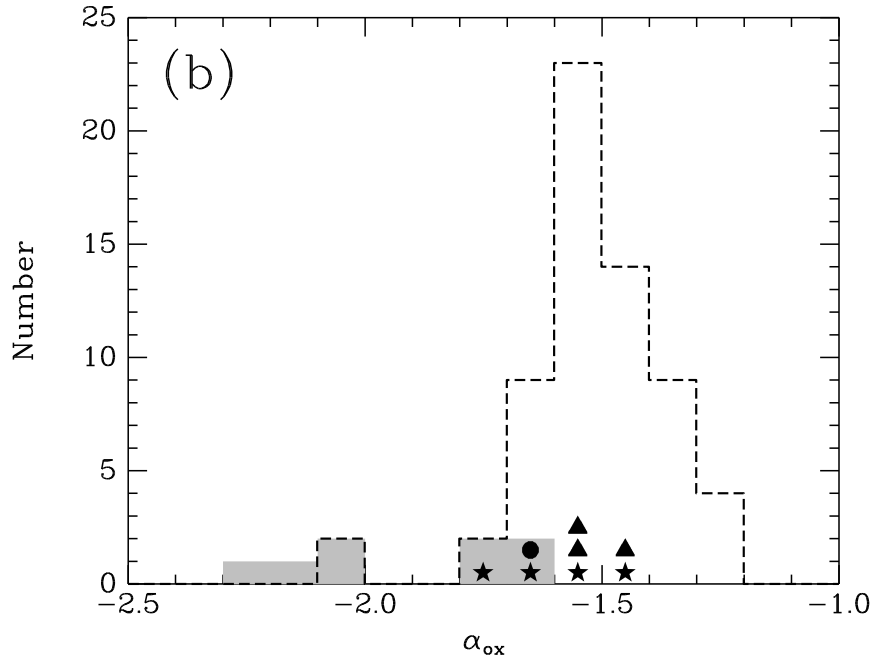
(b)
Number
25
20
15
10
5
0
−2.5
−2.0
−1.5
−1.0
α_{ox}

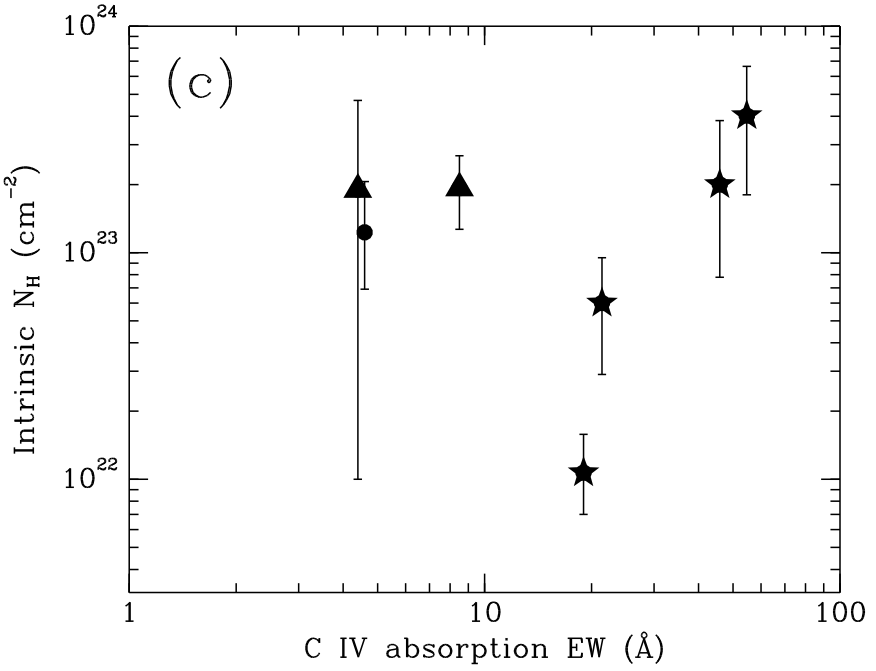
(c)
Intrinsic N_H (cm^{-2})
10^{24}
10^{23}
10^{22}
1
10
100
C IV absorption EW (Å)